Journal of Medicinal Chemistry

Article

pubs.acs.org/jmc

Discovery and Early Development of TMC647055, a Non-Nucleoside Inhibitor of the Hepatitis C Virus NS5B Polymerase

Maxwell D. Cummings,[†] Tse-I Lin,[‡] Lili Hu, Abdellah Tahri, David McGowan, Katie Amssoms, Stefaan Last, Benoit Devogelaere,[§] Marie-Claude Rouan, Leen Vijgen, Jan Martin Berke, Pascale Dehertogh, Els Fransen, Erna Cleiren, Liesbet van der Helm, Gregory Fanning, Origène Nyanguile,[∥] Kenny Simmen, Pieter Van Remoortere,[†] Pierre Raboisson, and Sandrine Vendeville*

Janssen Infectious Diseases BVBA (formerly Tibotec BVBA), Turnhoutseweg 30, 2340 Beerse, Belgium

Supporting Information

ABSTRACT: Structure-based macrocyclization of a 6-carboxylic acid indole chemotype has yielded potent and selective finger-loop inhibitors of the hepatitis C virus (HCV) NS5B polymerase. Lead optimization in conjunction with in vivo evaluation in rats identified several compounds showing (i) nanomolar potency in HCV replicon cells, (ii) limited toxicity and off-target activities, and (iii) encouraging preclinical pharmacokinetic profiles characterized by high liver distribution. This effort culminated in the identification of TMC647055 (**10a**), a nonzwitterionic 17-membered-ring macrocycle characterized by high affinity, long polymerase residence time, and broad genotypic coverage. In vitro results of the combination of **10a** with the HCV protease inhibitor TMC435 (simeprevir) supported an evaluation of this combination in patients with regard to virus suppression and resistance emergence. In a phase 1b trial with HCV genotype 1-infected patients, **10a** was considered to be safe and well-tolerated and demonstrated potent antiviral activity, which was further enhanced in a combination study with TMC435.

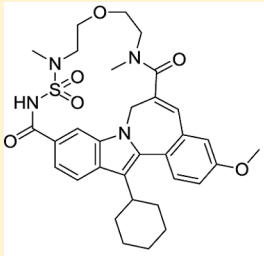

10a

EC_{50} = 77 nM

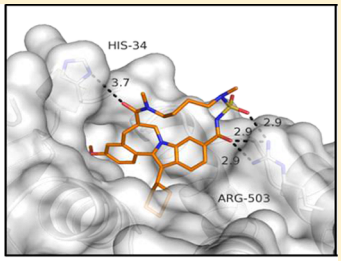

INTRODUCTION

Hepatitis C virus (HCV) represents a major global health burden and is associated with increased risk of liver cirrhosis and hepatocellular carcinoma, which is the leading cause of liver transplants in the USA.[1−3] Despite the availability of new therapies combining either of the recently approved direct-acting antiviral agents (DAAs) boceprevir[4,5] and telaprevir,[6,7] both of which are NS3 protease inhibitors, with PEGylated interferon α (as weekly injections) and ribavirin (b.i.d.), there remains a high medical need for new DAAs with complementary modes of action. Such regimens involving clinically validated protease inhibitors and inhibitors of the NS5B polymerase and the NS5A replication complex are needed in order to (i) increase cure rates, especially in difficult-to-treat patients; (ii) limit the development of resistant mutants; (iii) optimize the tolerability/side-effect profile; and (iv) decrease treatment duration. Ultimately, it is anticipated that combinations of several DAAs in an all-oral interferon-sparing regimen will lead to highly effective and better-tolerated treatments.

The NS5B polymerase plays an essential role in the life cycle of HCV since it is responsible for viral replication.[8,9] Two classes of polymerase inhibitors have shown proof-of-concept in clinical development: nucleoside analogues recognized by the active site and incorporated into nascent RNA as chain (or delayed chain) terminators[10,11] and non-nucleoside inhibitors (NNIs) binding to at least four distinct allosteric sites.[12−14] NNI-1 inhibitors, also called thumb domain 1 or finger-loop inhibitors, bind in a pocket distal to the catalytic site at the interface of the finger and thumb domains of the polymerase.[15−17] A 6-carboxylic acid indole chemotype represented by the early lead compound **1** (Figure 1)[18] was optimized by several groups based on two distinct strategies, both of which yielded clinical candidates. In the first strategy, extension from the carboxylic acid moiety and incorporation of rather large and charged diamide moieties, combined with the more metabolically stable cyclopentyl group rather than the cyclohexyl group, led to the clinical candidate BILB1941 (**2**) (Figure 1).[19] In the second strategy, conformational rigidification by introduction of a tether between the indole nitrogen and the C2-aryl group was explored, leading to tetracyclic and pentacyclic structures, most of which were zwitterions, as exemplified by MK-3281 (**3**) (Figure 1), a compound that reached human phase 1 clinical study.[20]

To avoid the possible formation of acyl glucuronide metabolites from the carboxylic acid group[21] (a potential cause of immunogenic reactions and toxicity[22−24]) and the

Special Issue: HCV Therapies

Received: September 10, 2013

   dx.doi.org/10.1021/jm401396p | J. Med. Chem. XXXX, XXX, XXX−XXX

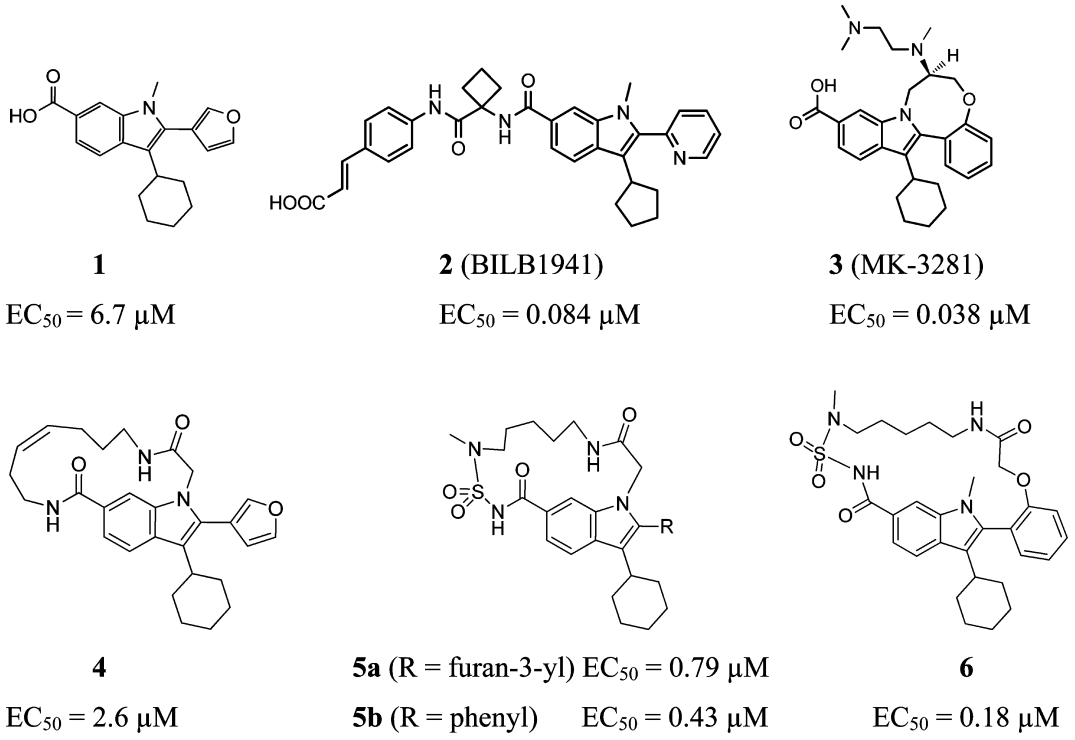

Figure 1. Structures of the early lead compound **1**, the clinical candidates **2** (BILB1941) and **3** (MK-3281), and initial 1,6- and 2,6-indole-based macrocycles **4**–**6**.

presence of a zwitterionic structure (a possible cause of exposure variability in patients[25]), we applied a structure-based macrocyclization strategy centered on the introduction of a linker in the solvent-exposed region, incorporating a carboxylic acid bioisostere. It was anticipated that this strategy would improve the permeability and avoid the formation of potentially toxic glucuronide acid derivatives as phase 2 metabolites while providing inhibitors with superior potency and pharmacokinetic (PK) profiles due to the effect of conformational restriction. Early crystal structures provided details on the binding mode of this chemotype to the NNI-1 site,[15,26] and we used this information to guide the initial exploration of three macrocycle classes. The first type of macrocycle, in which the linker is attached to the indole nitrogen and the C6 position of the indole via an amide, served as a proof-of-concept for this strategy, since micromolar potency was obtained in the replicon assay with macrocycle **4** (Figure 1) while its open precursor (prior to the ring-closure metathesis step) was completely inactive (not shown).[27] As expected, an acyl sulfamide replacement for the amide group proved to be a much better bioisostere of the carboxylic acid and provided macrocycles **5a** and **5b** with submicromolar EC_{50}'s of 0.79 and 0.43 μM, respectively. Similar findings were obtained for the second type of macrocycle, where the linker is attached to the C2 aryl group instead of the indole nitrogen in an effort to restrict the free rotation of the aryl moiety and favor the bioactive conformation. Thus, macrocycle **6** displayed an improved potency of 0.18 μM in the replicon assay. However, while most of our initial criteria, including cellular potency, no potential for acyl glucuronide formation, no zwitterion, and good bioavailability and distribution to the liver in rats after oral administration, had been satisfied with this second series of macrocycles, this series was still hampered by rather high in vivo clearance in rats despite moderate in vitro metabolic turnover in microsomes [clearances typically higher than 7 L h^{-1} kg^{-1} after IV administration of 2 mg/kg compound in 70:30 PEG400/saline]. We then concentrated our efforts on a third series of macrocycles in which the linker originates from a bridge and forms a seven-membered ring between the indole nitrogen and the C2 aryl group. Our subsequent optimization efforts involved the exploration of three types of bridge: saturated, unsaturated, and incorporating a cyclopropyl group.[28]

In this article, we describe the discovery of the macrocyclic indole TMC647055 (**10a**), which is currently being evaluated in phase 2 clinical trials in combination with TMC435 (simeprevir), a once-daily protease inhibitor discovered at Janssen during a research collaboration with Medivir. We review the synthesis, structure–activity relationships, and binding interactions of this new series of tetracyclic indole-based macrocycles, and we also discuss genotypic coverage, resistance, and mutant selection. The potential for combination with other DAAs and preliminary results in healthy volunteers and HCV genotype 1-infected patients, including those obtained in combination with TMC435,[29,30] are also presented.

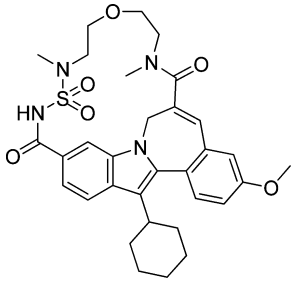

10a

dx.doi.org/10.1021/jm401396p | J. Med. Chem. XXXX, XXX, XXX–XXX

Scheme 1. Synthesis of 10a[a]

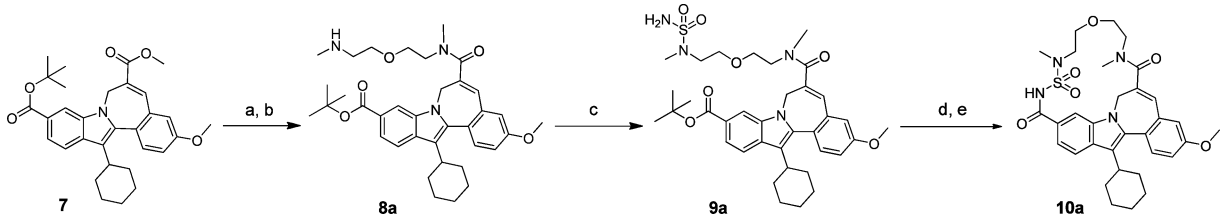

[a]Reagents and conditions: (a) NaOH, THF, H_2O, MeOH, RT (95%). (b) 2,2′-Oxybis(*N*-methylethanamine) (5 equiv), HATU, DIPEA, THF. (c) Sulfamide, dioxane, 100 °C. (d) TFA/DCM. (e) (i) CDI, dry THF, RT; (ii) DBU, THF.

CHEMISTRY

Macrocyclic indole derivatives **10a–i** were synthesized following a six-step procedure starting from the orthogonally protected bisester tetracycle **7**.[28] The synthetic route is exemplified with the structure of TMC647055 (**10a**) in Scheme 1. After hydrolysis of the methyl ester, a HATU-mediated amide coupling was performed using an excess of the symmetrical bisamine 2,2′-oxybis(*N*-methylethanamine) under diluted conditions in THF to give amide **8a** in 93% yield. A monoprotected unsymmetrical bisamine could also be used stoichiometrically and then further deprotected under acidic conditions (i.e., TFA in DCM for the removal of the Boc protecting group) or under basic conditions using thiophenol in the case of the nosyl protecting group. The free amino group was then converted to the sulfamide moiety using an excess of sulfamide in dioxane at 100 °C to give derivative **9a** in good yield (95%). The *tert*-butyl ester was subsequently cleaved under acidic conditions (TFA in DCM) in quantitative yield, and the ring closure was performed using a tandem of reactions involving activation of the carboxylic acid by CDI followed by intramolecular attack of the anion of the sulfamide group, formed by addition of DBU. This synthetic route yielded macrocycle **10a** in 49% overall yield from bisester **7** and was also used to synthesize macrocycles **10b–i**. Alternatively, ring closure could be performed by a HATU-mediated macrolactamization under high dilution after successive introduction of a sulfamide derivative containing a protected amine using the two-step CDI/DBU procedure described above and cleavage of the methyl ester and then the amino protecting group of the linker. Macrocycles **10j–l** were synthesized according to this latter route (not shown).[28]

Upon catalytic hydrogenation, compound **10a** gave a mixture of enantiomers that could be separated by chiral chromatography, yielding the enantiomerically pure macrocycles **11a** and **12a** containing a saturated bridge (Figure 2).[28] The enantiomeric excesses were 100% and 99.1%, respectively.

Derivatives with the cyclopropyl bridge were obtained by cyclopropanation of bisester indole **7** using trimethylsulfoxonium chloride in the presence of sodium hydride followed by enantiomeric separation of the pair of enantiomers obtained with the chiral auxiliary (*S*)-4-benzyl-2-oxazolidinone by column chromatography, which yielded diastereoisomers **14** and **15**, as depicted in Scheme 2. After removal of the chiral auxiliary under basic conditions, the reaction sequence used for the preparation of macrocyclic derivative **10a** was applied to carboxylic acids **16** and **17**, yielding the cyclopropyl-bridged macrocycles **18a** and **19a** with 100% ee. For the two pairs of enantiomers **11a**/**12a** and **18a**/**19a**, assignment of stereochemistry was based on antiviral data in conjunction with conformational analysis and modeled binding modes predicated on earlier NS5B–inhibitor complexes.[28,31] The rich set of available and relevant public structural data allowed for the straightforward construction of what were deemed to be relatively reliable binding models on the basis of the assumption of common binding modes for the corresponding features of the new inhibitors. This approach, while based on modeled structures, seemed quite reliable, and our later results with a macrocyclic inhibitor complex (discussed below) proved to be fully consistent with our earlier speculations on both stereochemical preference and macrocycle design.

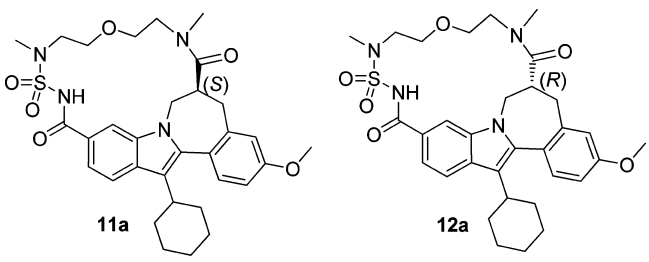

Figure 2. Structures of **11a** and **12a**.

The synthesis of macrocycle **25** with a "reduced" amide bond is outlined in Scheme 3. A one-pot procedure involving the conversion of carboxylic acid **20** to the corresponding isobutyl carbonate followed by sodium borohydride reduction afforded alcohol **21**. Subsequent introduction of the mesylate leaving group and its displacement by symmetrical *N*,*N*′-dimethyl-1,4-butanediamine allowed for the synthesis of intermediate **23**, which then underwent the same sequence of reactions as previously to yield the "reduced" macrocycle **25**.

SAR AND PK PROPERTIES LEADING TO THE SELECTION OF TMC647055

The anti-HCV potencies (EC_{50}'s) of compounds **10a–l**, **11a**, **12a**, **18a**, **19a**, and **25** were determined in the Huh-7 replicon cell line containing the subgenomic bicistronic HCV genotype 1b replicon clone ET and luciferase readout[29] (Table 1). In an effort to better understand the observed structure–activity relationship (SAR), and in the absence of a reliable permeability determination for this class of macrocycles,[32] binding affinities on the 1b polymerase were measured by surface plasmon resonance (SPR)[33] (Table 1). Cytotoxicity was measured in MT4 and Huh-7 cell lines and was minimal for all the compounds tested (CC_{50} > 25 μM). Studies with the unsaturated-bridged macrocyclic series revealed several structure–activity trends. The 16- and 17-membered macrocycles were optimal. An 18-membered analogue (**10b**) suffered a 2-fold decrease in replicon potency (cf. **10a** and **10c**) despite improved binding affinity (K_d = 0.8 nM). Smaller ring size

dx.doi.org/10.1021/jm401396p | J. Med. Chem. XXXX, XXX, XXX–XXX

Scheme 2. Synthesis of 18a and 19a[a]

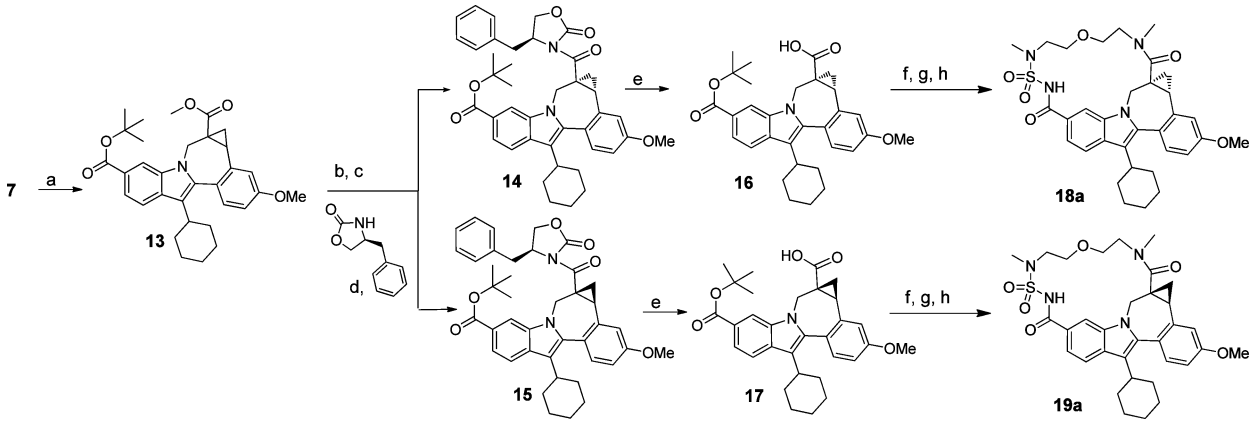

[a]Reagents and conditions: (a) (i) Trimethylsulfoxonium chloride, NaH, DMSO, RT; (ii) 7, 50 °C. (b) NaOH, H_2O/THF/MeOH, RT. (c) $(COCl)_2$, DMF, THF, 0 °C. (d) (*S*)-4-Benzyl-2-oxazolidinone (1.1 equiv), *n*-BuLi (1.1 equiv), THF, −78 °C. (e) NaOH (1 N), MeOH/THF, RT. (f) 2,2′-Oxybis(*N*-methylethanamine) (5 equiv), HATU, DIPEA,THF. (g) (i) Sulfamide, dioxane, 100 °C; (ii) TFA/DCM. (h) (i) CDI, dry THF, RT; (ii) DBU, THF.

Scheme 3. Synthesis of 25[a]

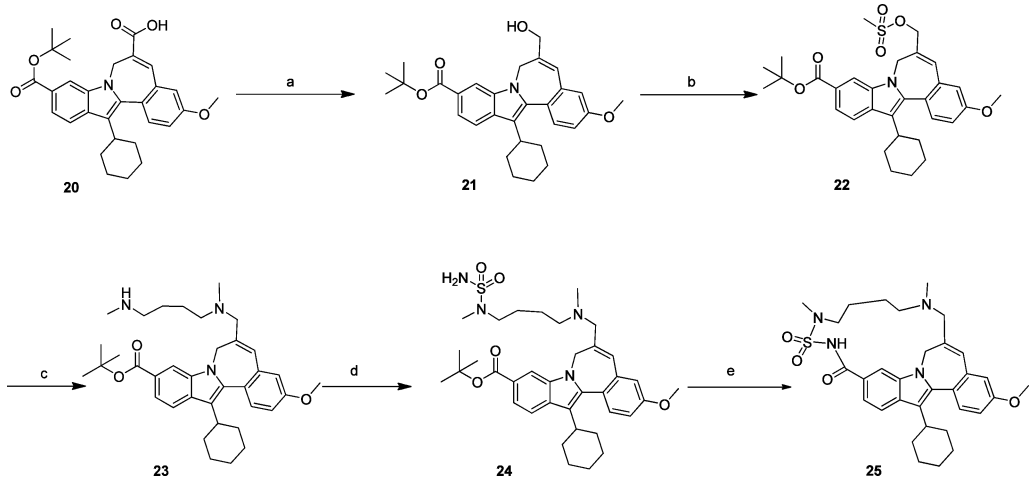

[a]Reagents and conditions: (a) *N*-Methylmorpholine, isobutyl chloroformate, THF, −15 °C, then $NaBH_4$, 0 °C. (b) Et_3N, $MeSO_2Cl$, THF, 0 °C. (c) *N*,*N*′-Dimethyl-1,4-butanediamine, THF, RT. (d) Sulfamide, dioxane, 105 °C. (e) (i) TFA, DCM, RT; (ii) CDI, acetonitrile, 60 °C; (iii) DBU, acetonitrile, RT.

(compound **10d**, 15-membered ring) led to decreased binding affinity and replicon potency. Ether and alkyl linkers were similarly potent, while the presence of a basic nitrogen in the linker decreased the activity (**10f** and the piperazine derivatives **10g** and **10l**), contrasting with earlier reports on non-macrocyclic indoles.[20] Substitution of the linker nitrogens had dramatic effects. Two methyl substituents proved optimal, while monomethyl analogues (**10j** and **10k**) were less potent in both binding and cellular assays, with an additional effect of decreased permeability for macrocycle **10j**. Derivatives with R^1 = methoxy (**10a**) and fluoro (**10i**) showed similar potencies, while R^1 = chloro (**10h**) gave a 4-fold loss of potency in the replicon assay, likely attributable to high lipophilicity in view of the good binding affinity (K_d = 1.5 nM) observed for this compound. While keeping the ether linker constant, the nature and stereospecificity of the seven-membered bridge was evaluated with the saturated analogues **11a** and **12a** and cyclopropyl-bridged macrocycles **18a** and **19a**. For these two subseries, only the *R* enantiomers (**12a** and **19a**) showed good antiviral activity, with 20- and 40-fold losses of potency for the less active enantiomers **11a** and **18a**, respectively. Saturation of the double bond yielded a compound with potency similar to that of the unsaturated analogue **10a** (EC_{50} = 79 and 77 nM for **12a** and **10a**, respectively), while cyclopropanation gave a 2-fold improvement (**19a**, EC_{50} = 40 nM). Figure 3 shows models of both enantiomers of a simple non-macrocyclic *N*,*N*-dimethylamide, highlighting the different trajectories accessible to this pair. In this case, the models have been adjusted to closely mimic the bound conformation observed for **10c** on which they are overlaid; under these (idealized) conditions it is clear that while the *R* amide overlays closely with that of bound **10c**, such a trajectory is not possible for the *S* enantiomer. Thus, we speculate that the less active *S* enantiomers are unable to adopt the optimal binding conformation within the constraint imposed by the 17-membered macrocycle. Extensive conformational adjustment involving the core indole−phenyl system of the inhibitor would be expected to have a profound and likely negative effect on the binding affinity. Additional changes in binding contacts could reasonably be expected for the contact with Arg503 as well as the contact with His34,

dx.doi.org/10.1021/jm401396p | J. Med. Chem. XXXX, XXX, XXX−XXX

Table 1. Effect of the Subseries, Linker, And Phenyl Substitution on Replicon Potency and Binding Affinity

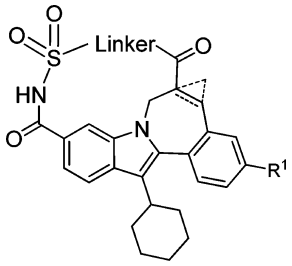

N°	Sub-series	R^1	Linker	EC_{50}[a] nM	K_d[b] nM
10a	unsaturated	OMe	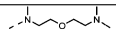	77	4.1
10b	unsaturated	OMe	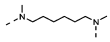	160	0.8
10c	unsaturated	OMe	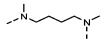	75	2.4
10d	unsaturated	OMe		680	7.0
10e	unsaturated	OMe	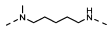	130	0.9
10f	unsaturated	OMe	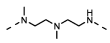	550	nd
10g	unsaturated	OMe	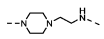	860	25.0
10h	unsaturated	Cl	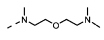	280	1.5
10i	unsaturated	F	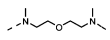	72	nd
10j	unsaturated	OMe		912	7.1
10k	unsaturated	OMe		550	15.0
10l	unsaturated	OMe	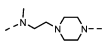	180	nd
11a	saturated (*S*)	OMe	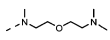	3830	nd
12a	saturated (*R*)	OMe	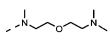	79	nd
18a	cyclopropyl (*S*)	OMe	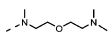	800	nd
19a	cyclopropyl (*R*)	OMe	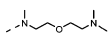	40	nd

[a]Replicon potency. [b]Dissociation constant determined by surface plasmon resonance with NS5B con1b(Δ21).[33]

which has been observed for bound **10c** (discussed below in Crystallography and Modeling).

Interestingly, the carbonyl of the amide group proved to be critical for potency, since the "reduced" macrocycle **25** exhibited a 30-fold decrease in cellular anti-HCV replicon activity relative to amide **10c** (EC_{50} = 2.34 μM versus 0.075 μM). The antiviral potency in the presence of 40% human serum was also measured, since this series of macrocycles generally exhibited high binding to plasma proteins in vitro (e.g., the free fraction of **10a** in the presence of plasma is 0.3%), which could limit the in vivo efficacy. The resulting serum shifts were generally 10−15-fold (9-fold for **10a**), with no clear SAR for this parameter. Rather than trying to decrease the serum shift, our strategy focused on the selection of compounds exhibiting high distribution to the liver, since HCV replication takes place almost exclusively in hepatocytes. We anticipated that this parameter could be an important contributor to the efficacy of compounds in patients[34,35] and that it may correspond to a more therapeutically relevant way of discriminating among inhibitors with relatively good anti-HCV replicon activities compared with the common strategy of minimizing the serum shift. Ultimately, a concentration in the liver at 7 h postdose that was higher than the serum-shifted EC_{50} was used as a criterion to select the most promising compounds.

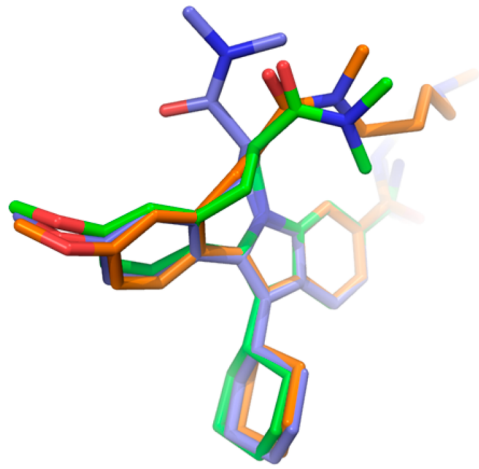

Figure 3. Stereospecificity of the saturated bridged system. Depicted are conformers of non-macrocyclic *N*,*N*-dimethylamide (*R*, green; *S*, purple), showing the stereospecific difference in the trajectory from the bridge, overlaid onto the NS5B-bound conformation of **10c** (orange).

A panel of analogues chosen for their good antiviral potency, acceptable in vitro metabolic stability, and chemical diversity, were then evaluated in vivo in Sprague−Dawley rats after IV and oral administration at 2 and 10 mg/kg, respectively. In addition to the classical PK parameters, concentrations in the liver at 7 h postdose were also measured (Table 2).

The nature of the bridge had a profound impact on the PK parameters, with the unsaturated analogue **10a** exhibiting the best overall profile, including good systemic absorption (bioavailability higher than 66%), high distribution to the liver (7800 ng/g, 7 h postdose), and moderate clearance. The saturated derivative **12a** showed clearance similar to that of **10a** but had low bioavailability and low distribution to the liver (15% and 898 ng/g, respectively), while the cyclopropyl derivative **19a** showed a relatively high clearance of 5.2 L h^{-1} kg^{-1}, in agreement with its low in vitro liver microsome stability (70% of the compound metabolized after 15 min in rat liver microsomes). The nature of the linker was also important: the unsubstituted amide derivative **10e** had good distribution to the liver but a poor absolute bioavailability of only 6%, highlighting the role of the amide substituent on permeability, while

dx.doi.org/10.1021/jm401396p | J. Med. Chem. XXXX, XXX, XXX−XXX

Table 2. Pharmacokinetic Parameters of Selected Macrocyclic Analogues (2 mg/kg IV, 10 mg/kg PO; Vehicle 70:30 PEG400/Saline IV, PEG400/2% vitE-TPGS PO; n = 3)

compd	HLM[a]	Cl (L h^{-1} kg^{-1})[b]	[liver] (ng/g)[c]	L/P[d]	F (%)[e]
10a	35	3.2	7800	46	>66
10c	56	2.4	5000	23	76
10e	32	4.2	6317	341	6
10i	38	3.7	6560	62	52
10l	26	9.4	299	108	3
12a	63	3.2	898	22	15
19a	95	5.2	3200	38	51

[a]Human liver microsomes stability, expressed as percentage of compound metabolized after 15 min at a concentration of 5 μM. [b]Plasma clearance. [c]Liver concentration after oral administration 7 h postdose. [d]Liver/plasma ratio after oral administration 7 h postdose. [e]Oral bioavailability.

macrocycle **10l** with a basic piperazine moiety showed an extremely poor overall profile, combining high clearance (despite good in vitro liver microsome metabolic stability), low absorption, and poor distribution to the liver. Finally, replacement of the methoxy group by a fluoro substituent (**10i**) led to PK properties similar to those of **10a**, as did replacement of the ether-containing linker by the alkyl linker (**10c**). On the basis of the overall good in vitro and in vivo properties, **10a** was further evaluated in dogs and showed an acceptable PK profile characterized by high oral bioavailability (F = 87%) and high systemic exposure (C_{max} = 10.2 μM and $AUC_{0-\infty}$ = 25.8 μM h) after a single 10 mg/kg oral dose, combined with moderate plasma clearance (Cl = 0.54 L h^{-1} kg^{-1}) and a low volume of distribution (Vd_{ss} = 0.32 L/kg).

CRYSTALLOGRAPHY AND MODELING

Macrocycle **10c**, a close structural analogue of TMC647055, was successfully cocrystallized with a ΔC_{21} construct of genotype 1b strain J4 NS5B (Figures 3–6).[31] The observed binding mode for the tetracyclic core and pendant cyclohexyl moiety of **10c** bound to the NNI-1 site of NS5B is consistent with those of the equivalent moieties of the previously published structures (PDB IDs 2BRK and 2BRL[15] and 2DXS[26]) that were used to guide our design strategy. The cyclohexyl ring and the corresponding hydrophobic edge of the relatively rigid indole–phenyl ring system sit in a hydrophobic pocket, while the opposite and relatively flexible side of the macrocycle (the macrocycle linker) is largely solvent-exposed. The acyl sulfamide moiety forms two hydrogen bonds with the guanidine of Arg503. Distinctively, the **10c** complex resolves additional N-terminal residues of the NNI-1 site in comparison with other published NNI-1 complexes (e.g., Figure 6);[15,26] interestingly, this difference may be due to a (weak) binding contact between the amide carbonyl of the macrocycle and His34 (Figure 4a).[31]

Molecular modeling analysis suggested that **10a** should be able to adopt a binding mode essentially identical to that of **10c**, possibly involving slight conformational adjustments in parts of the flexible macrocycle linker, which is one atom longer in **10a** (Figure 4b). The occupancy of the hydrophobic regions of the binding site and the multiple contacts with Arg503 are expected to be essentially identical to those described above for **10c**, whereas the contact with His34 is less clear because of the difference in the macrocycle linker lengths of **10c** and **10a**.

Binding of inhibitors at both the NNI-1 and NNI-2 sites displaces the fingertip Λ1 loop, a change that is thought to lock the enzyme in an inactive "open" state and thus lead to inhibition.[15,36] **10c** bound in the NNI-1 site closely mimics features of the fingertip Λ1 loop, positioning hydrophobic aryl groups similarly to the side chains of Leu30 and Leu31 of the bound loop (Figure 5) and effectively competing with the native intramolecular protein–protein interaction.

Since the original formulation of our macrocycle design strategy,[31] additional structures detailing indoles bound at the NNI-1 site have been disclosed.[20,37,38] These structures reveal additional information about feasible binding interactions in the NNI-1 site and are also consistent with previous structures. Figure 6 shows overlays of bound **10c** with two examples of these more recent indole inhibitors, and in both cases we see a tight overlay with the tetracyclic cyclohexyl–indole–phenyl core of bound **10c**. Similar to **10c**, the new structures show multiple hydrogen-bonding contacts with the guanidine of Arg503. The importance of this interaction was noted previously,[15,26,31] with earlier structures incorporating a carboxylate for this contact; one key element of our macrocycle design strategy was the replacement of this carboxylate. In our original report, we described the more buried pocket where the

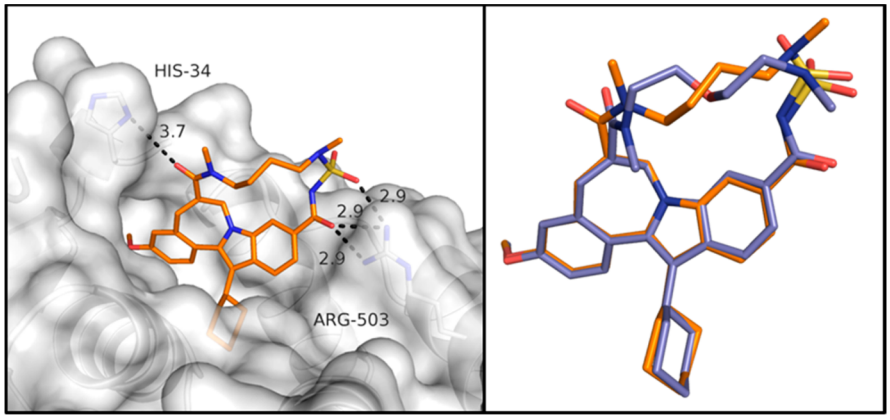

Figure 4. Observed and modeled binding modes. (A) Crystal structure of **10c** (orange) bound at the NNI-1 site, showing the pocket surface and details of contacts with His34 and Arg503. (B) Overlay of bound **10c** (orange) and the modeled low-energy conformer of **10a** (purple).

dx.doi.org/10.1021/jm401396p | J. Med. Chem. XXXX, XXX, XXX–XXX

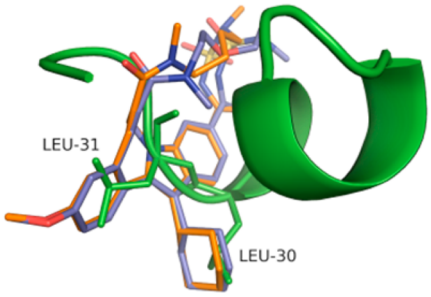

Figure 5. Comparison of bound inhibitors with the native NNI-1 site protein–protein interaction. Shown are bound **10c** and a model of **10a** (as in Figure 4b) overlaid on the NS5B loop that occupies NNI-1 in the absence of bound inhibitor [protein of the NNI-1 site is not shown; the loop is from monomer B of the **10c**–NS5B complex structure (PDB ID 4DRU)].[31]

methoxyphenyl moiety of bound **10c** sits, compared with the more exposed regions seen in earlier structures. This difference persists in the more recent structures, the two examples of which both show the more exposed pocket in this region of the binding site (Figure 6). The reason(s) for the observation of the more enclosed pocket in this region of the binding site in our structure remains unclear, but it may be due to the methoxyphenyl group that protrudes more deeply into the pocket and/or the weak contact between the inhibitor amide carbonyl and His34 mentioned above. Both of these chemical features are relatively unique to **10c** in comparison with the inhibitors bound at this site in other published structures.

PRECLINICAL CHARACTERIZATION OF TMC647055 (10A)

On the basis of the promising anti-HCV replicon activity and PK profiles in preclinical species, **10a** was selected as a candidate for clinical development, and its biological profile with respect to binding kinetics, genotypic coverage, resistance and mutant selection, combination with other DAAs, and preliminary safety were further characterized.[33]

10a elicited a mean IC_{50} of 34 nM in an RNA-dependent, RNA polymerase primer-dependent transcription assay and inhibited the replication of a genotype 1b replicon (clone ET) in the Huh7-Luc cell line with a median EC_{50} of 77 nM (luciferase readout). In Huh7-SG-1a, a stable genotype 1a cell line, the median EC_{50} value was 166 nM (qRT-PCR readout). The mean 50% cytotoxic concentrations in Huh7 and MT4 cells in luciferase reporter assays were 42.1 μM (n = 5) and 28.9 μM (n = 16), respectively. Cytotoxicity measurements on a panel of additional cell lines (MRC-5, HEK-293T, HepG2, and VeroE6 cells) all resulted in CC_{50} values in excess of 50 μM.[33]

The binding kinetics of **10a** were measured by SPR and showed a high-affinity interaction with NS5B across all genotypes (i.e., median K_d < 35 nM), except for genotype 2b, for which a more than 20-fold decrease in K_d was observed, mainly because of a higher dissociation rate (see Table 3). For genotype 1b, the association and dissociation constants were 2.2×10^4 M^{-1} s^{-1} and 8.9×10^{-5} s^{-1}, respectively, resulting in a K_d of 4 nM and a half-life of 130 min. This rather long inhibitor residence time may represent a distinctive advantage over other indole derivatives with regard to in vivo efficacy and target selectivity.[39,40] Broad cross-genotypic coverage of **10a** was also confirmed in a transient replicon assay using chimeric replicons containing the NS5B region derived from patient isolates (Table 3), with **10a** showing consistently high potencies against genotypes 1a, 1b, 3a, 4a, and 6a. Similar to previous reports describing NNI-1 inhibitors,[41,42] we observed a >200-fold reduction in potency against genotypes 2a and 2b (Table 3).

Table 3. Median Binding Affinities and Antiviral Activities of 10a against Different Genotypes, Using NS5B Purified Proteins from Clinical Isolates and a Transient Replicon Assay with Chimeric Replicons Containing the NS5B Region Derived from Patient Isolates, Respectively

genotype	K_d (M)	n^a	EC_{50} (μM)	n^a
wild-type 1b	4.1×10^{-9}		0.051	
1a	7.3×10^{-9}	5	0.048	14
1b	3.9×10^{-9}	5	0.027	10
2a	–		12.530	1
2b	8.8×10^{-7}	3	>28.000	2
3a	6.1×10^{-9}	3	0.088	2
4a	2.0×10^{-9}	3	0.097	1
5a	2.1×10^{-8}	1	–	
6a	3.0×10^{-8}	1	0.113	2

[a]Number of isolates. For n = 1 or 2, the observed value or the mean of the two observed values, respectively, is reported.

The susceptibility of **10a** was tested on different genotype 1b replicons harboring mutations in the NS5B polymerase located in the NNI-1 pocket (L392I, V494A, and P495L), also

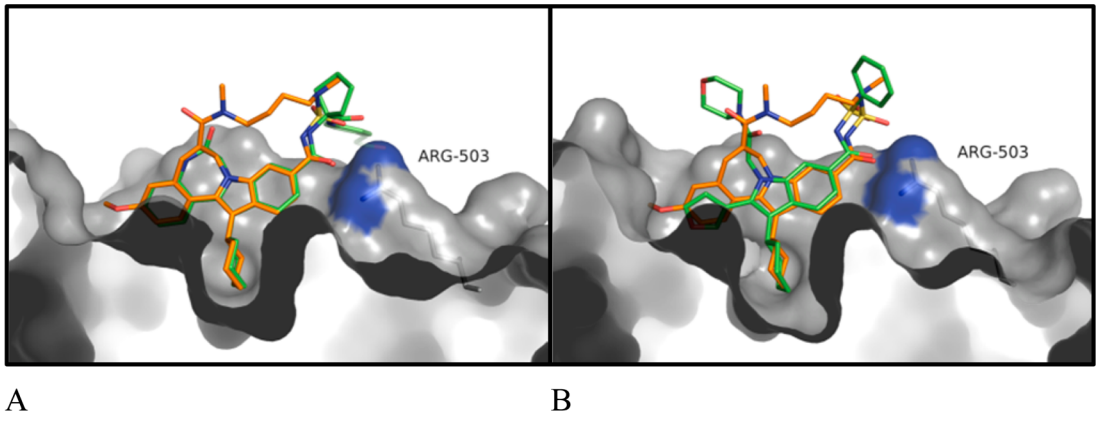

Figure 6. Comparison with recent NS5B NNI-1 complex structures. (A) **10c** with 3Q0Z (3Q0Z protein shown).[38] (B) **10c** with 4GMC (4GMC protein shown).[37]

dx.doi.org/10.1021/jm401396p | J. Med. Chem. XXXX, XXX, XXX–XXX

identified during in vitro resistance selection experiments with **10a**, and on other mutations outside of the NNI-1 pocket. The greatest decrease in antiviral potency, a 371-fold reduction in susceptibility relative to that of the wild-type genotype 1b replicon, was observed for the P495L mutant, consistent with previous reports identifying this position as a key mutation for NNI-1 site inhibitors.[16,33,42] The L392I and V494A mutations resulted in 9- and 3-fold median decreases, respectively, in anti-HCV replicon activity. Overall, these results mirror those of past resistance studies. Residues 392, 494, and 495 contribute to the NNI-1 site binding surface, making direct binding contacts with bound **10c**, **10a** (model shown in Figure 7), and

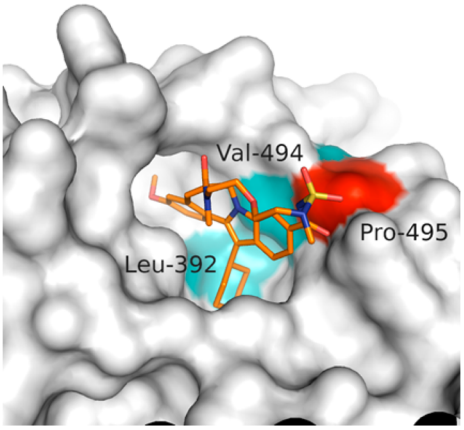

Figure 7. NS5B resistance mutations for **10a**. The **10a**–NS5B complex was modeled by superimposing a low-energy conformer of **10a** onto bound **10c** from the **10c**–NS5B complex, as shown in Figure 4b. Positions 392 (light teal), 494 (dark teal), and 495 (red) are highlighted.

other indoles that bind at this site.[15,20,26,37,38] Residue 392 contributes to the deepest part of the hydrophobic pocket occupied by the cyclohexyl moiety, while residue 494 contacts both the cyclohexyl ring and the face of the indole–phenyl system. Residue 495 packs against the face of the indole and is also near the critical acyl sulfamide moiety of the bound inhibitor; changes at this position are also likely to impact the positioning of Arg503, which forms multiple hydrogen bonds with bound **10c** and **10a** and makes similar interactions with other NNI-1 compounds. Thus, the resistance results seem consistent with the observed and modeled binding modes presented here. Additionally, the activity of **10a** was not affected by mutations associated with reduced sensitivity to NNI-2 (M423T), NNI-3 (M414T), NNI-4 (C316Y), HCV NS5B nucleoside/nucleotide inhibitors (S96T and S282T), HCV NS3/4A protease inhibitors (R155K, A156V, and D168V), and HCV NS5A inhibitors (L31V and Y93H).[33] NS3/4a inhibitors (e.g., TMC435) and NS5A inhibitors maintained full inhibitory potency against the NNI-1 mutants. This lack of cross-resistance suggested that combination therapy with other DAAs may be fruitful.

To further explore the effect of a combination of an NNI and a protease inhibitor on virus suppression and resistance development, an in vitro clearance and rebound experiment and a colony formation experiment were carried out with **10a** and TMC435 (Figure 8) using Huh7-Luc replicon cells.[33] In the clearance and rebound experiment, a 14 day incubation of the cells with the two inhibitors alone and in combination was followed by a 3 week "rebound" phase in the absence of

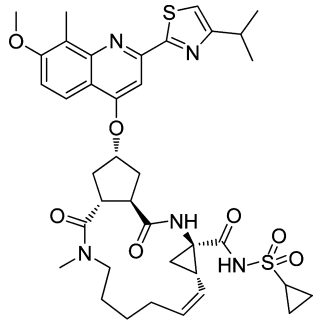

Figure 8. Structure of the HCV NS3/4A protease inhibitor TMC435 (simeprevir, Sovriad).

inhibitor. Complete clearance of replicon cells was achieved using the combination of 1.5 μM **10a** and 0.10 μM TMC435, while for each of these inhibitors alone, even at higher concentrations (3.75 and 0.25 μM for the NNI and protease inhibitors, respectively), incomplete clearance and rebound of replicon RNA was observed. In addition, in the colony formation experiments, in which Huh7-Luc replicon cells were incubated for 2–3 weeks with either TMC435 or **10a** or a combination of the two, the combination of these two inhibitors suppressed the formation of resistant colonies at low concentrations (0.75 and 0.08 μM for the NNI and protease inhibitor, respectively). At a higher concentration of 1.5 μM, **10a** alone led to a similar result, while the protease inhibitor (0.20 μM) alone did not.

The in vitro preliminary safety of **10a** was found to be acceptable in a battery of assays assessing cytotoxicity toward six different cell lines, genotoxicity, cardiovascular toxicity, selectivity versus human polymerases and a panel of enzymes and receptors, and potential reactivity with regard to glutathione adduct formation and acyl glucuronide formation. In addition, no systemic adverse effects were observed in a 5 day tolerance study with up to 1000 mg kg^{-1} day^{-1} in rat, except for a small decrease in body weight.

EARLY CLINICAL DEVELOPMENT OF TMC647055 (10A)

The safety and tolerability of **10a** after repeated administrations during 5 days and a morning dose at day 6 was demonstrated in healthy volunteers given oral b.i.d. doses of 300 mg, 1000 mg, and 1250 mg as well as in HCV genotype 1-infected patients given oral b.i.d. doses of 500 mg and 1000 mg. The most commonly reported adverse events were gastrointestinal (nausea, vomiting, loose stools, diarrhea, and abdominal cramps/discomfort), probably related to the hydroxypropyl-β-cyclodextrin vehicle. There were no serious adverse events (SAEs), no grade 3 or 4 AEs, and no clinically significant effects on laboratory parameters, vital signs, food consumption, appetite, or ECG profile. The main pharmacokinetic observations were (i) a marginal food effect, (ii) a slightly greater than dose-proportional increase in plasma concentrations in healthy volunteers and a dose-proportional increase in HCV-infected patients, (iii) an approximately 2-fold higher exposure in infected patients relative to healthy volunteers, and (iv) a decrease in exposure during the treatment. The plasma concentrations of 4-β-hydroxycholesterol, the endogenous biomarker for CYP3A4 induction, increased with increasing

dx.doi.org/10.1021/jm401396p | J. Med. Chem. XXXX, XXX, XXX–XXX

TMC647055 dose in healthy volunteers, indicating that TMC647055 induced CYP3A4 and its own metabolism. Mean trough concentrations in patients exceeded the replicon genotype 1a/1b EC_{50} values at both 500 and 1000 mg b.i.d. The antiviral response showed dose-dependent median maximum decreases in HCV RNA from baseline of 1.4 $\log_{10}$ and 2.4 $\log_{10}$ in GT1a patients with HCV RNA data available up to Day 6 at 500 and 1000 mg b.i.d., respectively. In GT1b patients, the median maximum decreases in HCV RNA were similar at the two dose levels (3.3 $\log_{10}$ at 500 mg b.i.d. and 3.4 $\log_{10}$ at 1000 mg b.i.d.).

These results encouraged further assessment of the combination of **10a** with the protease inhibitor TMC435, which had previously shown improved results in vitro relative to each of these compounds alone with regard to virus suppression and resistance development. The combination of **10a** (1000 mg b.i.d.) and TMC435 (150 mg q.d.) was given to HCV genotype 1a- and 1b-infected patients for 10 days and found to be safe and well-tolerated. Potent antiviral activity was measured, with a median HCV RNA decrease of 4.64 $\log_{10}$ IU/mL at day 11. The decline in plasma HCV RNA was substantially better than observed with either **10a** or TMC435 alone. Importantly, no viral breakthrough was detected, and no emerging mutations in the NNI-1 pocket of the polymerase associated with reduced in vitro sensitivity to **10a** were seen. However, emergence of the R155K mutation in the NS3/4A protease, which leads to a 30-fold decrease in susceptibility to TMC435,[43] was detected in six/seven genotype 1a-infected patients during dosing or at follow-up.[44] Finally, this combination was characterized by a decrease of the mean exposures of the two compounds upon repeated dosing, attributable to CYP3A4 induction by **10a**.

Because of the good safety and tolerability combined with potent antiviral activity, the combination of **10a** and TMC435 is being evaluated in an all-oral once-daily regimen with low-dose ritonavir to counterbalance the CYP3A4 induction, with and without ribavirin b.i.d., in a phase 2 interferon-free study.

CONCLUSION

A structure-based macrocyclization strategy was applied to a known 6-carboxylic acid indole chemotype, leading to the discovery of potent and selective inhibitors of HCV NS5B polymerase devoid of the undesirable features characterizing non-macrocyclic analogues (potential for acyl glucuronide formation and presence of zwitterions). Lead optimization focused on the subseries containing the more rigid bridged-indole macrocycles, in combination with early in vivo evaluation in rats, culminated rapidly in the discovery of the clinical candidate **10a**. This 17-membered-ring macrocycle is characterized by high affinity for and persistent binding to NS5B polymerase, encouraging in vivo properties in preclinical species (most notably high distribution to the liver in rats), and an acceptable preliminary safety profile. Furthermore, **10a** exhibits a favorable in vitro antiviral profile with respect to cross-genotypic coverage, virus suppression, and resistance selection, alone or in combination with the HCV NS3 protease inhibitor TMC435. These encouraging results translated to safe and well-tolerated treatment for HCV genotype 1-infected patients, demonstrating a strong antiviral effect that was more pronounced in combination treatment with TMC435. These results warrant further assessment of this combination in an all-oral once-daily interferon-free regimen with a low dose of ritonavir to optimize the pharmacokinetic−pharmacodynamic parameters.

EXPERIMENTAL SECTION

General Information. NMR spectra were recorded on a Bruker Avance 400 spectrometer operating at 400 MHz for ^{1}H. Chemical shifts are given in parts per million and *J* values in hertz. Multiplicities are indicated using the following abbreviations: s for singlet, d for doublet, t for triplet, m for multiplet, etc. Details on the different LC−MS methods used for the characterization of the new compounds described in this section (designated as LCMS-1 to LCMS-6 and HPLC-chiral) can be found in the Supporting Information. Chemical purities were >95% for all final compounds, as assessed by two LC−MS analysis methods.

1,1-Dimethylethyl 6-[[[2-[2-[(Aminosulfonyl)methylamino]-ethoxy]ethyl]methylamino]carbonyl]-13-cyclohexyl-3-methoxy-7*H*-indolo[2,1-*a*][2]benzazepine-10-carboxylate (9a). A solution of NaOH (6.38 g) in 25 mL of water was added to a stirred solution of bisester **7** (2 g, 3.9 mmol, synthesized as reported in ref 28) in THF (100 mL) and MeOH (150 mL). After 1 h, the reaction mixture (RM) was concentrated under reduced pressure and then diluted with ice-cold water (150 mL). The pH of the resulting solution was adjusted to 6 with acetic acid. The resulting precipitate was collected by filtration, washed with water, and dried under vacuum to give 1.90 g (98% yield) of 10-(1,1-dimethylethoxycarbonyl)-13-cyclohexyl-3-methoxy-7*H*-indolo[2,1-*a*][2]benzazepine-6-carboxylic acid (**20**) as a yellowish powder. To a stirred solution of carboxylic acid **20** (1.00 g, 2.05 mmol), DIPEA (1.07 mL, 6.15 mmol), and 2,2′-oxybis(*N*-methylethanamine) (1.08 g, 8.20 mmol) in 30 mL of dry THF was added HATU (1.17 g, 3.08 mmol) under nitrogen. After 1 h, the RM was quenched with water (100 mL) and extracted with ethyl acetate (75 mL). The organic layer was successively dried (Na_2SO_4), filtered, and evaporated. The residue was triturated in water, filtered off, and dried in a high-vacuum oven to give 1.15 g (93% yield) of 1,1-dimethylethyl 13-cyclohexyl-3-methoxy-6-[[methyl[2-[2-(methylamino)ethoxy]ethyl]amino]carbonyl]-7*H*-indolo[2,1-*a*][2]-benzazepine-10-carboxylate (**8a**) as a yellowish powder, which was used without any further purification in the next step. LCMS-1 95% pure, t_R = 3.03 min, *m/z* 602.4 $[M + H]^+$; HRMS (APPI+) calcd for $C_{36}H_{48}N_3O_5$ $[M + H]^+$ 602.3594, found 602.3578. A solution of **8a** (1.15 g, 1.91 mmol) and sulfamide (1.84 g, 19.1 mmol) in dioxane (10 mL) was heated at 100 °C in a microwave oven for 20 min. The RM was then cooled to RT and evaporated under vacuum. The residue was triturated in water, filtered off, and washed with water. The powder was redissolved in EtOAc, dried (Na_2SO_4), filtered, and evaporated to give 1.15 g (88% yield) of the desired product **9a** as a yellowish powder. LCMS-1 100%, t_R = 3.37 min, *m/z* 681.3 $[M + H]^+$; HRMS (APPI+) calcd for $C_{36}H_{49}N_4O_7$ $[M + H]^+$ 681.3322, found 681.3314; ^{1}H NMR (400 MHz, DMSO-d_6) δ 1.26−1.44 (m, 4H) 1.61 (s, 9H) 1.75 (d, *J* = 13.35 Hz, 2H) 1.84 (d, *J* = 13.35 Hz, 2H) 2.04 (qd, *J* = 12.55, 3.15 Hz, 2H) 2.70 (s, 3H) 2.86 (tt, *J* = 12.20, 3.60 Hz, 1H), 2.95 (s, 3H) 3.13 (t, *J* = 5.79 Hz, 2H) 3.49−3.56 (m, 6H) 3.91 (s, 3H) 4.69 (br s, 2H) 6.31 (br s, 2H) 6.97 (s, 1H) 7.13 (d, *J* = 2.77 Hz, 1H) 7.16 (dd, *J* = 8.56, 2.77 Hz, 1H) 7.55 (d, *J* = 8.56 Hz, 1H) 7.58 (dd, *J* = 8.56, 1.51 Hz, 1H) 7.84 (d, *J* = 8.31 Hz, 1H) 8.05 (d, *J* = 1.01 Hz, 1H).

2,19-Methano-3,7:4,1-dimetheno-1*H*,11*H*-14,10,2,9,11,17-benzoxathiatetraazacyclodocosine-8,18(9*H*,15*H*)-dione 27-Cyclohexyl-12,13,16,17-tetrahydro-22-methoxy-11,17-dimethyl-10,10-dioxide (10a). TFA (3.0 g, 26.3 mmol) was added to a solution of **9a** (1.15 g, 1.70 mmol) in dichloromethane (30 mL). After 1 h, the RM was concentrated under vacuum. The residue was triturated in ether, filtered, washed with ether, and then purified by chromatography (gradient EtOAc to EtOAc/EtOH 9:1) to give 802 mg (76% yield) of the carboxylic acid intermediate. LCMS-1 96%, t_R = 2.72 min, *m/z* 625 $[M + H]^+$; HRMS (APPI+) calcd for $C_{32}H_{41}N_4O_7S$ $[M + H]^+$ 625.2696, found 625.2683; ^{1}H NMR (400 MHz, DMSO-d_6) δ 1.22−1.50 (m, 4H) 1.75 (m, 3H) 1.83 (m, 2H) 1.96−2.12 (m, 2H) 2.70 (s, 3H) 2.80−2.91 (m, 1H) 2.94 (s, 3H) 3.13 (t, *J* = 5.92 Hz, 2H) 3.47−3.58 (m, 6H) 3.90 (s, 3H) 4.68 (br s, 2H) 6.32 (br s, 2H) 6.96 (s, 1H) 7.12 (d, *J* = 2.77 Hz, 1H) 7.16 (dd, *J* = 8.56, 2.77 Hz, 1H)

dx.doi.org/10.1021/jm401396p | J. Med. Chem. XXXX, XXX, XXX−XXX

7.54 (d, J = 8.56 Hz, 1H) 7.63 (dd, J = 8.31, 1.26 Hz, 1H) 7.83 (d, J = 8.31 Hz, 1H) 8.10 (s, 1H). Carbonyldiimidazole (389 mg, 2.40 mmol) was added to a stirred solution of the previous intermediate (500 mg, 0.80 mmol) in dry THF (8 mL). The RM was stirred at RT for 1 h and then concentrated, and the resulting residue was purified by flash chromatography (gradient EtOAc to CH_3CN 1:0 to 0:1) to give 550 mg of the acylimidazole intermediate as a slightly yellow solid. HRMS (APPI+) calcd for $C_{35}H_{43}N_6O_6S$ $[M + H]^+$ 675.2965, found 675.2950. DBU (244 mg, 0.32 mmol) was added to a solution of the acylimidazole (550 mg) in acetonitrile (25 mL). The RM was stirred overnight at RT and then concentrated under reduced pressure. The residue was dissolved in water (30 mL), and the pH of the resulting solution was adjusted to 5 with acetic acid. The precipitate was collected by filtration, washed with water, and dried. Recrystallization from ethanol followed by column chromatography purification (gradient EtOAc to EtOAc/EtOH 9:1) provided 380 mg (78% yield) of the title product **10a** as a white powder. LCMS-1 99.6%, t_R = 3.81 min, m/z 607 $[M + H]^+$, LCMS-2 100%, t_R = 1.02 min; HRMS (APPI$^+$) calcd for $C_{32}H_{39}N_4O_6S$ $[M + H]^+$ 607.2590, found 607.2609; ^{1}H NMR (DMSO-d_6) δ 1.15 (m, 1H) 1.40 (m, 3H) 1.71 (m, 2H) 1.88 (m, 1H) 2.01 (m, 3H) 2.56 (m, 3H) 2.77 (m, 1H) 2.99 (s, 3H) 3.26 (m, 2H) 3.50−3.71 (m, 6H) 3.87 (s, 3H) 4.44 (d, J = 14.1 Hz, 1H) 5.09 (d, J = 15.0 Hz, 1H) 6.95 (s, 1H) 7.13 (s, 1H) 7.19 (d, J = 8.6 Hz, 1H) 7.47 (d, J = 8.0 Hz, 1H) 7.54 (d, J = 8.3 Hz, 1H) 7.88 (d, J = 7.8 Hz, 1H) 8.33 (s, 1H) 11.40 (s, 1H).

(19*S*)-2,19-Methano-3,7:4,1-dimetheno-1*H*,11*H*-14,10,2,9,11,17-benzoxathiatetraazacyclodocosine-8,18-(9*H*,15*H*)-dione 27-Cyclohexyl-12,13,16,17,19,20-hexahydro-22-methoxy-11,17-dimethyl-10,10-dioxide (11a) and (19*R*)-2,19-Methano-3,7:4,1-dimetheno-1*H*,11*H*-14,10,2,9,11,17-benzoxathiatetraazacyclodocosine-8,18(9*H*,15*H*)-dione 27-Cyclohexyl-12,13,16,17,19,20-hexahydro-22-methoxy-11,17-dimethyl-10,10-dioxide (12a). A solution of **10a** (56 mg, 0.092 mmol) in MeOH (15 mL) and THF (5 mL) was hydrogenated in an H-cube apparatus using a 10% Pd on carbon cartridge. Then the solvent was evaporated, and the residue was purified by column chromatography (CH_2Cl_2/CH_3CN 9:1) to give 23 mg (41% yield) of the desired saturated product as a racemic mixture, which was further separated by SFC using a 6.5 min run on a chiral CHIRALCEL OD-H column (250 × 10 mm, coated on 5 μm silica gel) with 55% methanol/45% CO_2 as the mobile phase at a flow rate of 10 mL/min to give the two pure enantiomers **11a** and **12a**. Retention times under these conditions were observed at 4.25 and 5.54 min, respectively. Compound **11a**: HPLC-chiral 99.57%, t_R = 2.80 min, ee = 99.1%; LCMS-3 99.7%, t_R = 5.12 min, m/z 609 $[M + H]^+$. Compound **12a**: HPLC-chiral 100%, t_R = 2.27 min, ee = 100%; LCMS-3 99.7%, t_R = 5.12 min, m/z 609 $[M + H]^+$; ^{1}H NMR (400 MHz, DMSO-d_6) δ 1.15−1.30 (m, 1H) 1.32−1.46 (m, 2H) 1.55−1.81 (m, 3H) 1.82−2.09 (m, 4H) 2.54−2.59 (m, 1H) 2.79−2.91 (m, 1H) 2.92−3.09 (m, 5H) 3.34−3.49 (m, 6H) 3.51−3.60 (m, 1H) 3.64−3.74 (m, 2H) 3.76−3.96 (m, 6H) 4.53 (d, J = 14.81 Hz, 1H) 6.98−7.11 (m, 2H) 7.32 (m, 2H) 7.75−7.88 (m, 2H) 11.30 (br s, 1H).

(4b*S*,5a*R*)-*tert*-Butyl 5a-((*S*)-4-Benzyl-2-oxooxazolidine-3-carbonyl)-12-cyclohexyl-3-methoxy-4b,5,5a,6-tetrahydrobenzo[3,4]cyclopropa[5,6]azepino[1,2-*a*]indole-9-carboxylate (14) and (4b*R*,5a*S*)-*tert*-Butyl 5a-((*S*)-4-Benzyl-2-oxooxazolidine-3-carbonyl)-12-cyclohexyl-3-methoxy-4b,5,5a,6-tetrahydrobenzo[3,4]cyclopropa[5,6]azepino[1,2-*a*]indole-9-carboxylate (15). Sodium hydride (1.54 g, 64 mmol) was added to a stirred suspension of trimethylsulfoxonium chloride (9.07 g, 2.2 equiv) in anhydrous DMSO (100 mL) under nitrogen. After 30 min at RT, 16 g (32 mmol, 1 equiv) of neat bisester **7** was added portionwise. After 2 h at RT, TLC showed completion of the reaction, and the RM was quenched with water. The resulting precipitate was filtered off, washed with water, and dried in the vacuum oven. Purification by flash chromatography on silica gel (gradient of MeOH in DCM) provided 9.5 g (57% yield) of the desired cyclopropyl intermediate **13** as a racemic mixture. Subsequent cleavage of the methyl ester using the same procedure as described for the synthesis of **20** gave the corresponding carboxylic acid in 95% yield as a light-yellow solid. At 0 °C under a protective atmosphere, oxalyl chloride (4.07 mL, 47.4 mmol) was added to a solution of the previous carboxylic acid intermediate (19.83 g, 39.5 mmol) and DMF (5 drops) in dry tetrahydrofuran (100 mL). Upon addition of oxalyl chloride, the immediate formation of gas was observed. The RM was stirred at 0 °C for 1.5 h. Then an additional 0.5 equiv of oxalyl chloride was added, and the RM was stirred for 1 h (repeated once until full conversion was obtained). The RM was evaporated to dryness in vacuo to afford 20.5 g (97% yield) of the acid chloride as a white solid, which was used directly in the next step. To a solution of (*S*)-4-benzyl-2-oxazolidinone (7.50 g, 42.3 mmol) in dry tetrahydrofuran (60 mL) under a nitrogen atmosphere, *n*-butyllithium (26.4 mL, 42.3 mmol) was added slowly at −78 °C. The RM was stirred for 40 min at −78 °C. After 40 min, the anion solution was added via a cannula to a solution of the acid chloride (20 g, 38.5 mmol) in 60 mL of THF at −78 °C. The RM was stirred for 1.5 h at −78 °C. When the reaction was finished, it was quenched with an ammonium chloride solution at −70 °C. The RM was then warmed to RT, extracted with EtOAc, washed with brine, and dried over Na_2SO_4. The organic layer was filtered and concentrated to afford 26.34 g of a yellow solid. The two enantiomers **14** and **15** were separated by flash column chromatography using 5:1 heptane/EtOAc (the faster-running spot corresponded to **15**) and were obtained as light-yellow solids with a purity of 97% in yields of 85% (11.17 g) and 81% (10.6 g), respectively; m/z 661 $[M + H]^+$.

(4b*R*,5a*S*)-9-(*tert*-Butoxycarbonyl)-12-cyclohexyl-3-methoxy-4b,5,5a,6-tetrahydrobenzo[3,4]cyclopropa[5,6]azepino-[1,2-*a*]indole-5a-carboxylic Acid (17). Diastereoisomer **15** (11.17 g, 16.90 mmol) was first dissolved in THF (130 mL), and then methanol (130 mL) was added. A 1 N NaOH solution (101 mL, 101 mmol) was added slowly to keep the temperature below 30 °C. The RM was stirred at RT for 2 h. When the reaction was finished, 1 N HCl solution was added until the pH reached 2. Water (500 mL) was then added, and the RM was extracted with EtOAc, washed with brine, and concentrated. Purification by flash column chromatography using 1:1 heptane/EtOAc afforded 5.24 g (60% yield) of the desired carboxylic acid **17** with an ee of 97%. ^{1}H NMR (400 MHz, DMSO-d_6, mixture of rotamers, 60/40 major/minor) δ 1.08−1.26 (m, 2H) 1.27−1.48 (m, 8H) 1.51−1.62 (m, 20H) 1.66−1.79 (m, 4H) 1.81−2.11 (m, 8H) 2.65−2.92 (m, 4H) 3.41−3.44 (m, 1H major) 3.85 (s, 3H major) 3.86 (s, 3H minor) 3.95 (d, J = 15.19 Hz, 1H minor) 5.12 (d, J = 15.19 Hz, 1H minor) 5.35 (d, J = 14.74 Hz, 1H major) 6.99−7.08 (m, 2H) 7.17−7.31 (m, 4H) 7.52 (dd, J = 8.47, 1.43 Hz, 1H major) 7.60 (dd, J = 8.58, 1.32 Hz, 1H minor) 7.79 (d, J = 8.58 Hz, 1H major) 7.85 (d, J = 8.36 Hz, 1H minor) 7.97 (d, J = 0.88 Hz, 1H minor) 8.26 (d, J = 1.10 Hz, 1H major).

(1a*R*,12b*S*)-8-Cyclohexyl-11-methoxy-16,22-dimethyl-1,12b-dihydro-5,1a-(methanoiminothioiminoethanooxy-ethanoiminomethano)cyclopropa[*d*]indolo[2,1-*a*][2]benz-azepine-13,23(2*H*)-dione 15,15-Dioxide (19a). This macrocycle was synthesized following the same sequence of reactions as described for the synthesis of the unsaturated macrocyclic analogue **10a**, starting from carboxylic acid **17** instead of **20**, and was obtained as a white solid. LCMS-5 100%, t_R = 6.57 min; LCMS-6 100%, t_R = 1.90 min; HPLC-chiral 100%, t_R = 5.00 min, ee = 100%; ^{1}H NMR (400 MHz, DMSO-d_6, 100 °C) δ 1.21−2.08 (m, 12H) 2.48−2.51 (m, 1H) 2.82−3.90 (m, 16H) 5.13 (d, J = 15.34 Hz, 1H) 7.01 (dd, J = 8.48, 2.83 Hz, 1H) 7.08−7.17 (m, 1H) 7.28 (d, J = 8.48 Hz, 1H) 7.38 (dd, J = 8.48, 1.21 Hz, 1H) 7.77 (d, J = 8.48 Hz, 1H) 8.04 (d, J = 1.21 Hz, 1H) 10.93 (br s, 1H).

(1a*S*,12b*R*)-8-Cyclohexyl-11-methoxy-16,22-dimethyl-1,12b-dihydro-5,1a-(methanoiminothioiminoethanooxy-ethanoiminomethano)cyclopropa[*d*]indolo [2,1-*a*][2]benz-azepine-13,23(2*H*)-dione 15,15-Dioxide (18a). This macrocycle was synthesized following the same sequence of reactions as described for the synthesis of the other enantiomer **19a**, starting from diastereoisomer **14** instead of **15**, and was obtained as a white solid. LCMS-5 100%, t_R = 6.56 min; LCMS-6 100%, t_R = 1.90 min; HPLC-chiral 100%, t_R = 4.62 min, ee = 100%; ^{1}H NMR (400 MHz, DMSO-d_6) δ 1.13−2.14 (m, 12H) 2.45 (t, J = 7.26 Hz, 1H) 2.75−3.90 (m, 16H) 5.11 (d, J = 15.19 Hz, 1H) 7.05 (dd, J = 8.47, 2.53 Hz, 1H) 7.13 (d, J = 2.20 Hz, 1H) 7.26 (d, J = 8.36 Hz, 1H) 7.28−7.35 (m, 1H) 7.79 (d, J = 8.36 Hz, 1H) 8.01−8.22 (m, 1H) 11.34 (s, 1H).

dx.doi.org/10.1021/jm401396p | J. Med. Chem. XXXX, XXX, XXX−XXX

1,1-Dimethylethyl 13-Cyclohexyl-6-hydroxymethyl-3-methoxy-7*H*-indolo[2,1-*a*][2]benzazepine-10-carboxylate (21). To a stirred solution of acid **20** (1300 mg, 2.67 mmol) and *N*-methylmorpholine (270 mg, 2.67 mmol) in dry THF (10 mL) was added dropwise at −15 °C isobutyl chloroformate (364 mg, 2.67 mmol), and the mixture was stirred at −15 °C for 15 min. The RM turned from yellow to orange. The suspension was filtered, and $NaBH_4$ (202 mg, 5.33 mmol) was added at 0 °C to the filtrate, followed by 2 drops of water. The RM was stirred in an ice bath for 2 h and then diluted with water and extracted with EtOAc. The organic phase was washed with water until neutral, dried ($MgSO_4$), filtered, and evaporated under vacuum. Purification by flash chromatography (heptane/EtOAc 9:1 to 1:1) gave 1 g (78% yield) of the desired alcohol **21** as a slightly yellow solid. LCMS-1 99.17%, t_R = 3.58 min, m/z 474 $[M + H]^+$; ^1H NMR (400 MHz, $CDCl_3$) δ 1.24−1.29 (m, 1H) 1.32−1.46 (m, 2H) 1.63 (s, 9H) 1.66−1.72 (m, 1H) 1.73−1.82 (m, 2H) 1.87−2.17 (m, 4H) 2.76−2.93 (m, 1H) 3.89 (s, 3H) 4.10−4.28 (m, 1H) 4.35 (br s, 2H) 4.74−4.99 (m, 1H) 6.68 (s, 1H) 6.88 (d, J = 2.35 Hz, 1H) 6.99 (dd, J = 8.61, 2.54 Hz, 1H) 7.48 (d, J = 8.61 Hz, 1H) 7.68 (d, J = 8.41 Hz, 1H) 7.83 (d, J = 8.41 Hz, 1H) 8.12 (s, 1H).

1,1-Dimethylethyl 13-Cyclohexyl-3-methoxy-6-[[(methylsulfonyl)oxy]methyl]-7*H*-indolo[2,1-*a*][2]-benzazepine-10-carboxylate (22). To a solution of alcohol **21** (500 mg, 1.056 mmol, 1.0 equiv) in THF (10 mL) were added Et_3N (160 mg, 1.5 equiv) and methanesulfonyl chloride (181 mg, 1.5 equiv) at 0 °C. The resulting solution was stirred at 0 °C for 2 h. The RM was then quenched with water and extracted with EtOAc. The organic layer was washed with water two times, dried over $MgSO_4$, filtered, and concentrated to give 555 mg (90% yield) of mesyl alcohol **22** as a yellow solid, which was used without further purification in the next step. LCMS-3 99%, t_R = 6.46 min, m/z 552 $[M + H]^+$; ^1H NMR (400 MHz, $CDCl_3$) δ 1.22−1.29 (m, 1H) 1.31−1.47 (m, 2H) 1.53−1.67 (m, 10H) 1.70−1.82 (m, 2H) 1.90−2.15 (m, 4H) 2.72−2.90 (m, 4H) 3.89 (br s, 3H) 4.19−4.41 (m, 1H) 4.77−4.87 (m, 1H) 4.92 (br s, 2H) 6.84 (br s, 1H) 6.89 (br s, 1H) 6.99−7.10 (m, 1H) 7.49 (d, J = 8.61 Hz, 1H) 7.70 (d, J = 8.41 Hz, 1H) 7.80−7.87 (m, 1H) 8.15 (br s, 1H).

1,1-Dimethylethyl 13-Cyclohexyl-6-[methyl[4-(methylamino)butyl]amino]methyl-3-methoxy-7*H*-indolo[2,1-*a*][2]benzazepine-10-carboxylate (23). To *N*,*N*′-dimethyl-1,4-butanediamine (105 mg, 5 equiv) dissolved in THF (5 mL) was added mesyl alcohol **22** (100 mg, 0.181 mmol) at RT. The RM was stirred at RT for 48 h and then diluted with water and extracted with EtOAc. The organic layer was dried ($MgSO_4$), filtered, and concentrated to give 450 mg (96% yield) of compound **23** as a slightly yellow solid, which was used without further purification in the next step. LCMS-1 99%, t_R = 3.64 min (broad peak), m/z 572 $[M + H]^+$; ^1H NMR (400 MHz, $CDCl_3$) δ 1.20−1.26 (m, 1H) 1.36−1.40 (m, 2H) 1.59 (s, 12H) 1.68−1.80 (m, 2H) 1.81−1.97 (m, 2H) 1.97−2.14 (m, 7H) 2.18−2.33 (m, 2H) 2.41 (s, 3H) 2.44−2.58 (m, 2H) 2.74−2.93 (m, 1H) 3.10 (br s, 2H) 3.90 (s, 3H) 3.99−4.11 (m, 1H) 4.94−5.19 (m, 1H) 6.55 (s, 1H) 6.81−6.90 (m, 1H) 6.91−7.02 (m, 1H) 7.48 (d, J = 8.41 Hz, 1H) 7.67 (d, J = 8.61 Hz, 1H) 7.76−7.85 (m, 1H) 8.16 (s, 1H).

1,1-Dimethylethyl 13-Cyclohexyl-6-[[methyl[4-[(aminosulfonyl)methylamino]butyl]amino]methyl]-3-methoxy-7*H*-indolo[2,1-*a*][2]benzazepine-10-carboxylate (24). A mixture of compound **23** (400 mg, 0.7 mmol) and sulfamide (336 mg, 5 equiv) in dioxane (20 mL) was heated at 105 °C. After 3 h, the RM was cooled to RT, concentrated in vacuum, redissolved in DCM, extracted with water, dried over $MgSO_4$, filtered, and concentrated. Purification by flash chromatography (DCM to EtOAc) gave 350 mg (63%) of compound **24** as a white foam. LCMS-1 100%, t_R = 3.18 min, m/z 651 $[M + H]^+$; ^1H NMR (400 MHz, $CDCl_3$) δ 1.22−1.52 (m, 7H) 1.62 (s, 9H) 1.69−1.82 (m, 2H) 1.83−2.15 (m, 8H) 2.21−2.34 (m, 2H) 2.78 (s, 3H) 2.80−2.91 (m, 1H) 3.01−3.18 (m, 4H) 3.90 (s, 3H) 4.01−4.16 (m, 1H) 4.64 (br s, 2H) 5.08 (m, 1H) 6.55 (s, 1H) 6.87 (s, 1H) 6.93−7.02 (m, 1H) 7.47 (d, J = 8.61 Hz, 1H) 7.65 (d, J = 7.82 Hz, 1H) 7.82 (d, J = 8.61 Hz, 1H) 8.10−8.17 (m, 1H).

11*H*-2,18-Methano-3,7:4,1-dimetheno-10,2,9,11,16-benzothiatetraazacycloheneicosine-8(9*H*,12*H*)-one 26-Cyclohexyl-13,14,15,16,17-pentahydro-21-methoxy-11,16-dimethyl-10,10-dioxide (25). To a solution of *tert*-butyl ester **24** (310 mg, 0.476 mmol) in DCM was added TFA (3.2 g, 60 equiv) at RT. The RM immediately turned yellow upon addition of TFA. After 2 h, the RM was concentrated to dryness, and the residue was triturated in diisopropyl ether. The resulting cream solid was filtered off and dried under high vacuum to give 350 mg (100% yield) of the corresponding carboxylic acid, which was used directly in the next step as a TFA salt. LCMS-1 98.5%, t_R = 2.39 min, m/z 595 $[M + H]^+$. To the carboxylic acid intermediate (TFA salt) dissolved in acetonitrile (20 mL) was added CDI (88 mg, 1.1 equiv) at RT. The RM was then heated at 50 °C for 2 h, at which time LC−MS showed complete conversion of the carboxylic acid to the acylimidazole intermediate. The RM was then diluted with ACN (50 mL), and DBU (225 mg, 3 equiv) was added at RT. After 16 h, the RM was quenched with diluted HCl (pH 2), concentrated in vacuum, and extracted with DCM. The organic layer was washed with water (until the water layer reached neutral pH), dried over $MgSO_4$, filtered, and concentrated under vacuum. The residue was triturated in DCM, and the resulting cream solid was filtered off to give 146 mg (46% yield) of compound **25**. LCMS-2 98%, t_R = 1.28 min, m/z 577 $[M + H]^+$; LCMS-4 100%, t_R = 1.51 min; ^1H NMR (400 MHz, DMSO-d_6) δ 1.06−1.21 (m, 1H) 1.24−1.51 (m, 8H) 1.60−2.09 (m, 8H) 2.13−2.28 (m, 1H) 2.55−2.68 (m, 1H) 2.70−2.84 (m, 2H) 3.02 (s, 3H) 3.10−3.22 (m, 1H) 3.36−3.49 (m, 2H) 3.85 (s, 3H) 4.08 (d, J = 13.80 Hz, 1H) 5.11 (d, J = 13.80 Hz, 1H) 6.65 (s, 1H) 7.02 (d, J = 2.51 Hz, 1H) 7.10 (dd, J = 8.78, 2.76 Hz, 1H) 7.35 (d, J = 8.28 Hz, 1H) 7.49 (d, J = 8.53 Hz, 1H) 7.82 (d, J = 8.53 Hz, 1H) 8.14 (s, 1H) 11.50 (br s, 1H).

■ ASSOCIATED CONTENT

Supporting Information

Details of LCMS and chiral HPLC methods. This material is available free of charge via the Internet at http://pubs.acs.org.

■ AUTHOR INFORMATION

Corresponding Author

*Phone: + 32 14 64 17 84. E-mail: svendev1@its.jnj.com.

Present Addresses

[†]Janssen Research & Development, Welsh and McKean Roads, Spring House, PA 19477, USA.

[‡]Roche R&D China Ltd., 720 Ca iLun Rd., Building 5, Pudong, 201203 Shanghai, P. R. China.

[§]Cartagenia, Technologie laan 3, 3001 Leuven, Belgium.

[∥]University of Applied Sciences and Arts Western Switzerland, Institute of Life Technologies, t_Re du Rawyl 47, 1950 Sion 2, Switzerland.

Notes

The authors declare no competing financial interest.

■ ACKNOWLEDGMENTS

We thank the analytical chemistry team for their technical assistance.

■ REFERENCES

(1) El-Serag, H. B. Hepatocellular carcinoma. *N. Engl. J. Med.* **2011**, *365*, 1118−1127.

(2) Ghany, M. G.; Strader, D. B.; Thomas, D. L.; Seeff, L. B. American Association for the Study of Liver, D. Diagnosis, management, and treatment of hepatitis C: An update. *Hepatology* **2009**, *49*, 1335−1374.

(3) The Global Burden of Hepatitis, C. W. G. Global Burden of Disease (GBD) for Hepatitis C. *J. Clin. Pharmacol.* **2004**, *44*, 20−29.

(4) Bacon, B. R.; Gordon, S. C.; Lawitz, E.; Marcellin, P.; Vierling, J. M.; Zeuzem, S.; Poordad, F.; Goodman, Z. D.; Sings, H. L.; Boparai, N.; Burroughs, M.; Brass, C. A.; Albrecht, J. K.; Esteban, R. Boceprevir for previously treated chronic HCV genotype 1 infection. *N. Engl. J. Med.* **2011**, *364*, 1207−1217.

(5) Poordad, F.; McCone, J.; Bacon, B. R.; Bruno, S.; Manns, M. P.; Sulkowski, M. S.; Jacobson, I. M.; Reddy, K. R.; Goodman, Z. D.; Boparai, N.; DiNubile, M. J.; Sniukiene, V.; Brass, C. A.; Albrecht, J. K.; Bronowicki, J.-P. Boceprevir for untreated chronic HCV genotype 1 infection. *N. Engl. J. Med.* **2011**, *364*, 1195−1206.
(6) Jacobson, I. M.; McHutchison, J. G.; Dusheiko, G.; Di Bisceglie, A. M.; Reddy, K. R.; Bzowej, N. H.; Marcellin, P.; Muir, A. J.; Ferenci, P.; Flisiak, R.; George, J.; Rizzetto, M.; Shouval, D.; Sola, R.; Terg, R. A.; Yoshida, E. M.; Adda, N.; Bengtsson, L.; Sankoh, A. J.; Kieffer, T. L.; George, S.; Kauffman, R. S.; Zeuzem, S. Telaprevir for previously untreated chronic hepatitis C virus infection. *N. Engl. J. Med.* **2011**, *364*, 2405−2416.
(7) Zeuzem, S.; Andreone, P.; Pol, S.; Lawitz, E.; Diago, M.; Roberts, S.; Focaccia, R.; Younossi, Z.; Foster, G. R.; Horban, A.; Ferenci, P.; Nevens, F.; Mullhaupt, B.; Pockros, P.; Terg, R.; Shouval, D.; van Hoek, B.; Weiland, O.; Van Heeswijk, R.; De Meyer, S.; Luo, D.; Boogaerts, G.; Polo, R.; Picchio, G.; Beumont, M. Telaprevir for retreatment of HCV infection. *N. Engl. J. Med.* **2011**, *364*, 2417−2428.
(8) Behrens, S. E.; Tomei, L.; De Francesco, R. Identification and properties of the RNA-dependent RNA polymerase of hepatitis C virus. *EMBO J.* **1996**, *15*, 12−22.
(9) Lohmann, V.; Korner, F.; Herian, U.; Bartenschlager, R. Biochemical properties of hepatitis C virus NS5B RNA-dependent RNA polymerase and identification of amino acid sequence motifs essential for enzymatic activity. *J. Virol.* **1997**, *71*, 8416−8428.
(10) Carroll, S. S.; Olsen, D. B. Nucleoside analog inhibitors of hepatitis C virus replication. *Infect. Disord.: Drug Targets* **2006**, *6*, 17−29.
(11) Jonckers, T. H. M.; Lin, T.-I.; Buyck, C.; Lachau-Durand, S.; Vandyck, K.; Van Hoof, S.; Vandekerckhove, L. A. M.; Hu, L.; Berke, J. M.; Vijgen, L.; Dillen, L. L. A.; Cummings, M. D.; de Kock, H.; Nilsson, M.; Sund, C.; Rydegard, C.; Samuelsson, B.; Rosenquist, A.; Fanning, G.; Van Emelen, K.; Simmen, K.; Raboisson, P. 2′-Deoxy-2′-spirocyclopropylcytidine revisited: A new and selective inhibitor of the hepatitis C virus NS5B polymerase. *J. Med. Chem.* **2010**, *53*, 8150−8160.
(12) Beaulieu, P. L. Non-nucleoside inhibitors of the HCV NS5B polymerase: Progress in the discovery and development of novel agents for the treatment of HCV infections. *Curr. Opin. Invest. Drugs* **2007**, *8*, 614−634.
(13) Koch, U.; Narjes, F. Allosteric inhibition of the hepatitis C virus NS5B RNA dependent RNA polymerase. *Infect. Disord.: Drug Targets* **2006**, *6*, 31−41.
(14) Tramontano, E. The exploding field of the HCV polymerase non-nucleoside inhibitors: Summary of first generation compounds. *Mini-Rev. Med. Chem.* **2008**, *8*, 1298−1310.
(15) Di Marco, S.; Volpari, C.; Tomei, L.; Altamura, S.; Harper, S.; Narjes, F.; Koch, U.; Rowley, M.; De Francesco, R.; Migliaccio, G.; Carfi, A. Interdomain communication in hepatitis C virus polymerase abolished by small molecule inhibitors bound to a novel allosteric site. *J. Biol. Chem.* **2005**, *280*, 29765−29770.
(16) Kukolj, G.; McGibbon, G. A.; McKercher, G.; Marquis, M.; Lefebvre, S.; Thauvette, L.; Gauthier, J.; Goulet, S.; Poupart, M.-A.; Beaulieu, P. L. Binding site characterization and resistance to a class of non-nucleoside inhibitors of the hepatitis C virus NS5B polymerase. *J. Biol. Chem.* **2005**, *280*, 39260−39267.
(17) Tomei, L.; Altamura, S.; Bartholomew, L.; Biroccio, A.; Ceccacci, A.; Pacini, L.; Narjes, F.; Gennari, N.; Bisbocci, M.; Incitti, I.; Orsatti, L.; Harper, S.; Stansfield, I.; Rowley, M.; De Francesco, R.; Migliaccio, G. Mechanism of action and antiviral activity of benzimidazole-based allosteric inhibitors of the hepatitis C virus RNA-dependent RNA polymerase. *J. Virol.* **2003**, *77*, 13225−13231.
(18) Beaulieu, P. L.; Gillard, J.; Bykowski, D.; Brochu, C.; Dansereau, N.; Duceppe, J. S.; Hache, B.; Jakalian, A.; Lagace, L.; LaPlante, S.; McKercher, G.; Moreau, E.; Perreault, S.; Stammers, T.; Thauvette, L.; Warrington, J.; Kukolj, G. Improved replicon cellular activity of non-nucleoside allosteric inhibitors of HCV NS5B polymerase: From benzimidazole to indole scaffolds. *Bioorg. Med. Chem. Lett.* **2006**, *16*, 4987−4993.
(19) Beaulieu, P. L.; Bos, M.; Cordingley, M. G.; Chabot, C.; Fazal, G.; Garneau, M.; Gillard, J. R.; Jolicoeur, E.; LaPlante, S.; McKercher, G.; Poirier, M.; Poupart, M. A.; Tsantrizos, Y. S.; Duan, J.; Kukolj, G. Discovery of the first thumb pocket 1 NS5B polymerase inhibitor (BILB 1941) with demonstrated antiviral activity in patients chronically infected with genotype 1 hepatitis C virus (HCV). *J. Med. Chem.* **2012**, *55*, 7650−7666.
(20) Narjes, F.; Crescenzi, B.; Ferrara, M.; Habermann, J.; Colarusso, S.; Ferreira, M. d. R. R.; Stansfield, I.; Mackay, A. C.; Conte, I.; Ercolani, C.; Zaramella, S.; Palumbi, M.-C.; Meuleman, P.; Leroux-Roels, G.; Giuliano, C.; Fiore, F.; Di Marco, S.; Baiocco, P.; Koch, U.; Migliaccio, G.; Altamura, S.; Laufer, R.; De Francesco, R.; Rowley, M. Discovery of (7*R*)-14-cyclohexyl-7-{[2-(dimethylamino)ethyl]-(methyl)amino}-7,8-dihydro-6*H*-indolo[1,2-*e*][1,5]benzoxazocine-11-carboxylic acid (MK-3281), a potent and orally bioavailable finger-loop inhibitor of the hepatitis C virus NS5B polymerase. *J. Med. Chem.* **2011**, *54*, 289−301.
(21) Giuliano, C.; Fiore, F.; Di Marco, A.; Padron Velazquez, J.; Bishop, A.; Bonelli, F.; Gonzalez-Paz, O.; Marcucci, I.; Harper, S.; Narjes, F.; Pacini, B.; Monteagudo, E.; Migliaccio, G.; Rowley, M.; Laufer, R. Preclinical pharmacokinetics and metabolism of a potent non-nucleoside inhibitor of the hepatitis C virus NS5B polymerase. *Xenobiotica* **2005**, *35*, 1035−1054.
(22) Bailey, M. J.; Dickinson, R. G. Acyl glucuronide reactivity in perspective: Biological consequences. *Chem.-Biol. Interact.* **2003**, *145*, 117−137.
(23) Castillo, M.; Smith, P. C. Disposition and reactivity of ibuprofen and ibufenac acyl glucuronides in vivo in the rhesus monkey and in vitro with human serum albumin. *Drug Metab. Dispos.* **1995**, *23*, 566−572.
(24) Skonberg, C.; Olsen, J.; Madsen, K. G.; Hansen, S. H.; Grillo, M. P. Metabolic activation of carboxylic acids. *Expert Opin. Drug Metab. Toxicol.* **2008**, *4*, 425−438.
(25) Zhao, Y. H.; Abraham, M. H.; Le, J.; Hersey, A.; Luscombe, C. N.; Beck, G.; Sherborne, B.; Cooper, I. Rate-limited steps of human oral absorption and QSAR studies. *Pharm. Res.* **2002**, *19*, 1446−1457.
(26) Ikegashira, K.; Oka, T.; Hirashima, S.; Noji, S.; Yamanaka, H.; Hara, Y.; Adachi, T.; Tsuruha, J.-I.; Doi, S.; Hase, Y.; Noguchi, T.; Ando, I.; Ogura, N.; Ikeda, S.; Hashimoto, H. Discovery of conformationally constrained tetracyclic compounds as potent hepatitis C virus NS5B RNA polymerase inhibitors. *J. Med. Chem.* **2006**, *49*, 6950−6953.
(27) McGowan, D.; Vendeville, S.; Lin, T. I.; Tahri, A.; Hu, L.; Cummings, M. D.; Amssoms, K.; Berke, J. M.; Canard, M.; Cleiren, E.; Dehertogh, P.; Last, S.; Fransen, E.; Van Der Helm, E.; Van den Steen, I.; Vijgen, L.; Rouan, M. C.; Fanning, G.; Nyanguile, O.; Van Emelen, K.; Simmen, K.; Raboisson, P. Finger-loop inhibitors of the HCV NS5b polymerase. Part 1: Discovery and optimization of novel 1,6- and 2,6-macrocyclic indole series. *Bioorg. Med. Chem. Lett.* **2012**, *22*, 4431−4436.
(28) Vendeville, S.; Lin, T. I.; Hu, L.; Tahri, A.; McGowan, D.; Cummings, M. D.; Amssoms, K.; Canard, M.; Last, S.; Van den Steen, I.; Devogelaere, B.; Rouan, M. C.; Vijgen, L.; Berke, J. M.; Dehertogh, P.; Fransen, E.; Cleiren, E.; van der Helm, L.; Fanning, G.; Van Emelen, K.; Nyanguile, O.; Simmen, K.; Raboisson, P. Finger-loop inhibitors of the HCV NS5b polymerase. Part II. Optimization of tetracyclic indole-based macrocycle leading to the discovery of TMC647055. *Bioorg. Med. Chem. Lett.* **2012**, *22*, 4437−4443.
(29) Lin, T.-I.; Lenz, O.; Fanning, G.; Verbinnen, T.; Delouvroy, F.; Scholliers, A.; Vermeiren, K.; Rosenquist, A.; Edlund, M.; Samuelsson, B.; Vrang, L.; de Kock, H.; Wigerinck, P.; Raboisson, P.; Simmen, K. In vitro activity and preclinical profile of TMC435350, a potent hepatitis C virus protease inhibitor. *Antimicrob. Agents Chemother.* **2009**, *53*, 1377−1385.
(30) Raboisson, P.; de Kock, H.; Rosenquist, A.; Nilsson, M.; Salvador-Oden, L.; Lin, T.-I.; Roue, N.; Ivanov, V.; Wahling, H.; Wickstrom, K.; Hamelink, E.; Edlund, M.; Vrang, L.; Vendeville, S.; Van de Vreken, W.; McGowan, D.; Tahri, A.; Hu, L.; Boutton, C.; Lenz, O.; Delouvroy, F.; Pille, G.; Surleraux, D.; Wigerinck, P.;

Samuelsson, B.; Simmen, K. Structure−activity relationship study on a novel series of cyclopentane-containing macrocyclic inhibitors of the hepatitis C virus NS3/4A protease leading to the discovery of TMC435350. *Bioorg. Med. Chem. Lett.* **2008**, *18*, 4853−4858.

(31) Cummings, M. D.; Lin, T. I.; Hu, L.; Tahri, A.; McGowan, D.; Amssoms, K.; Last, S.; Devogelaere, B.; Rouan, M. C.; Vijgen, L.; Berke, J. M.; Dehertogh, P.; Fransen, E.; Cleiren, E.; van der Helm, L.; Fanning, G.; Van Emelen, K.; Nyanguile, O.; Simmen, K.; Raboisson, P.; Vendeville, S. Structure-based macrocyclization yields hepatitis C virus NS5B inhibitors with improved binding affinities and pharmacokinetic properties. *Angew. Chem., Int. Ed.* **2012**, *51*, 4637−4640.

(32) Apparent permeability was assessed in caco-2 cells and was found to be unpredictive for in vivo absorption. For example, **10a** was predicted to be poorly absorbed with a P_{AB} of 2.8 cm/s but showed a very good exposure in rats and dogs. We postulate that our acyl sulfamide derivatives are mostly present in a charged form (anion) at the pH of the caco-2 cells experiment (pH 7.4), thus underestimating their permeability in the stomach and intestines where the pH is lower. For **10a**, the measured pK_a of the acidic acyl sulfamide moiety was 5.7.

(33) Devogelaere, B.; Berke, J. M.; Vijgen, L.; Dehertogh, P.; Fransen, E.; Cleiren, E.; van der Helm, L.; Nyanguile, O.; Tahri, A.; Amssoms, K.; Lenz, O.; Cummings, M. D.; Clayton, R. F.; Vendeville, S.; Raboisson, P.; Simmen, K. A.; Fanning, G. C.; Lin, T.-I. TMC647055, a potent non-nucleoside hepatitis C virus NS5B polymerase inhibitor with cross-genotypic coverage. *Antimicrob. Agents Chemother.* **2012**, *56*, 4676−4684.

(34) Lamarre, D.; Anderson, P. C.; Bailey, M.; Beaulieu, P.; Bolger, G.; Bonneau, P.; Bos, M.; Cameron, D. R.; Cartier, M.; Cordingley, M. G.; Faucher, A.-M.; Goudreau, N.; Kawai, S. H.; Kukolj, G.; Lagace, L.; LaPlante, S. R.; Narjes, H.; Poupart, M.-A.; Rancourt, J.; Sentjens, R. E.; St George, R.; Simoneau, B.; Steinmann, G.; Thibeault, D.; Tsantrizos, Y. S.; Weldon, S. M.; Yong, C.-L.; Llinàs-Brunet, M. An NS3 protease inhibitor with antiviral effects in humans infected with hepatitis C virus. *Nature* **2003**, *426*, 186−189.

(35) Liverton, N. J.; Holloway, M. K.; McCauley, J. A.; Rudd, M. T.; Butcher, J. W.; Carroll, S. S.; DiMuzio, J.; Fandozzi, C.; Gilbert, K. F.; Mao, S.-S.; McIntyre, C. J.; Nguyen, K. T.; Romano, J. J.; Stahlhut, M.; Wan, B.-L.; Olsen, D. B.; Vacca, J. P. Molecular modeling based approach to potent P2−P4 macrocyclic inhibitors of hepatitis C NS3/4A protease. *J. Am. Chem. Soc.* **2008**, *130*, 4607−4609.

(36) Biswal, B. K.; Cherney, M. M.; Wang, M.; Chan, L.; Yannopoulos, C. G.; Bilimoria, D.; Nicolas, O.; Bedard, J.; James, M. N. Crystal structures of the RNA-dependent RNA polymerase genotype 2a of hepatitis C virus reveal two conformations and suggest mechanisms of inhibition by non-nucleoside inhibitors. *J. Biol. Chem.* **2005**, *280*, 18202−18210.

(37) Beaulieu, P. L.; Coulombe, R.; Gillard, J.; Brochu, C.; Duan, J.; Garneau, M.; Jolicoeur, E.; Kuhn, P.; Poupart, M.-A.; Rancourt, J.; Stammers, T. A.; Thavonekham, B.; Kukolj, G. Allosteric *N*-acetamide-indole-6-carboxylic acid thumb pocket 1 inhibitors of hepatitis C virus NS5B polymerase—Acylsulfonamides and acyl sulfamides as carboxylic acid replacements. *Can. J. Chem.* **2013**, *91*, 66−81.

(38) Zheng, X.; Hudyma, T. W.; Martin, S. W.; Bergstrom, C.; Ding, M.; He, F.; Romine, J.; Poss, M. A.; Kadow, J. F.; Chang, C. H.; Wan, J.; Witmer, M. R.; Morin, P.; Camac, D. M.; Sheriff, S.; Beno, B. R.; Rigat, K. L.; Wang, Y. K.; Fridell, R.; Lemm, J.; Qiu, D.; Liu, M.; Voss, S.; Pelosi, L.; Roberts, S. B.; Gao, M.; Knipe, J.; Gentles, R. G. Syntheses and initial evaluation of a series of indolo-fused heterocyclic inhibitors of the polymerase enzyme (NS5B) of the hepatitis C virus. *Bioorg. Med. Chem. Lett.* **2011**, *21*, 2925−2929.

(39) Copeland, R. A.; Pompliano, D. L.; Meek, T. D. Drug-target residence time and its implications for lead optimization. *Nat. Rev. Drug Discovery* **2006**, *5*, 730−739.

(40) An optimized indole acetamide lead from the acyclic series (see ref 21) was found to have a half-life of 3 min in our in-house SPR experiment.

(41) Pauwels, F.; Mostmans, W.; Quirynen, L. M.; van der Helm, L.; Boutton, C. W.; Rueff, A. S.; Cleiren, E.; Raboisson, P.; Surleraux, D.; Nyanguile, O.; Simmen, K. A. Binding-site identification and genotypic profiling of hepatitis C virus polymerase inhibitors. *J. Virol.* **2007**, *81*, 6909−6919.

(42) Rydberg, E. H.; Cellucci, A.; Bartholomew, L.; Mattu, M.; Barbato, G.; Ludmerer, S. W.; Graham, D. J.; Altamura, S.; Paonessa, G.; De Francesco, R.; Migliaccio, G.; Carfi, A. Structural basis for resistance of the genotype 2b hepatitis C virus NS5B polymerase to site A non-nucleoside inhibitors. *J. Mol. Biol.* **2009**, *390*, 1048−1059.

(43) Lenz, O.; Verbinnen, T.; Lin, T.-I.; Vijgen, L.; Cummings, M. D.; Lindberg, J.; Berke, J. M.; Dehertogh, P.; Fransen, E.; Scholliers, A.; Vermeiren, K.; Ivens, T.; Raboisson, P.; Edlund, M.; Storm, S.; Vrang, L.; de Kock, H.; Fanning, G. C.; Simmen, K. A. In vitro resistance profile of the hepatitis C virus NS3/4A protease inhibitor TMC435. *Antimicrob. Agents Chemother.* **2010**, *54*, 1878−1887.

(44) Bourgeois, S.; Reesink, H. W.; Leempoels, J.; Vijgen, L.; Rouan, M.-C.; Marien, K.; Remoortere, P. V.; Fanning, G.; Picchio, G.; Simmen, K.; Verloes, R. Combination Therapy of TMC647055 with Simeprevir (TMC435) in Genotype 1 HCV Patients. EASL, The International Liver Conference, Amsterdam, 2013.